Integrated model for predicting the flexural capacity of concrete elements reinforced with non-corrodible discrete reinforcements

Tiago Valente[1], Christoph de Sousa[1], Inês Costa, Felipe Melo[1] and Joaquim Barros[2]

[1] CiviTest-Pesquisa de Novos Materiais para a Engenharia Civil, Lda., Vila Nova de Famalicão, Portugal
[2] ISISE, Institute of Science and Innovation for Bio-Sustainability (IB-S), Department of Civil Engineering, University of Minho, 4800-058, Guimarães, Portugal
tiagovalente@civitest.com

Abstract.
The present work describes an integrated approach that leads to the development of a new model capable of describing the tensile behavior (mode I) of fiber reinforced concrete (FRC), considering the orientation of the fibers, the fibers segregation along the cross-section of the FRC members and the pullout constitutive model of each fiber bridging the two faces of a crack.
The possibility of the numerical model to capture the flexural behavior of non-metallic fiber reinforced concrete members is explored by simulating the response of polypropylene fiber reinforced concrete notched beams submitted to 3-point bending tests.

Keywords: Polypropylene fibers; fiber reinforced concrete; flexural capacity.

1 Introduction

The use of short and randomly distributed fibers increases concrete's post-cracking tensile capacity, its ductility, energy absorption capacity and impact resistance when compared to plain concrete [1, 2]. Additionally, the restrain to crack opening, provided by the different fiber reinforcement mechanisms at fracture, enhances the durability and integrity of cement based materials. The fundamental reinforcement mechanism of fibers consists in the capacity of ensuring relatively high stress transfer between the faces of cracks, by restraining the degeneration of micro-cracks in meso- and macro-cracks, which increases the stiffness and load carrying capacity of concrete structures in their cracking stage, as well as their durability [3–6].

The fiber contribution after cracking depends mainly on the content of fibers, their orientation and distribution towards the potential cracks [7–10], the material and geometric characteristics of the fibers [11–13], and the quality of the concrete [14], which are designated as the variables that mainly affect the fiber reinforcement mechanisms. The present work presents the main aspects of an integrated model to predict the tensile behavior (mode I) of fiber reinforced concrete (FRC) by considering these variables in the form of a fiber orientation profile model, a fiber segregation model

and a fiber pullout constitutive model. It is believed that the followed approach can simulate more realistically the post-cracking response of FRC in comparison to the already available models, e.g. cohesive stress-crack width constitutive law.

Considering that the proposed model has already shown good agreement to simulate the flexural behavior of steel fiber reinforced concrete elements [15], the present work explores the potential of the model to capture the behavior of non-metallic fiber reinforcements, as is the case of polypropylene fibers (PP).

PP fibers have been used mainly in non-structural applications for limiting crack width due to shrinkage effects of cement-based materials. Being non-susceptible to corrosion, PP fibers can also be regarded as viable discrete reinforcement elements for the production of thin concrete elements. The relatively low elasticity modulus, tensile strength and almost frictional-based reinforcing nature of PP fibers have been pointed out as the main arguments for preventing their use in structural applications, as a total or even partial replacement of conventional steel reinforcements. However, significant improvements have been made, not only on the material properties of PP fibers, but also on their surface treatment, that provide the means to develop fiber reinforced concrete (FRC) with toughness levels capable of being used for structural applications, according to the requirements of fib Model Code 2010.

2 Integrated model for predicting flexural capacity of FRC structural elements

In order to predict the flexural capacity of FRC members, a numerical tool was developed that considers the influence of the orientation and segregation of fibers along the cross-section of the FRC members and the pullout constitutive law of each fiber bridging the two faces of a crack.

The integrated model was implemented in *DOCROS*, an already existing software for the analysis of cross-sections of R-FRC members failing in bending [16]. In *DOCROS* a cross-section is discretized in N layers, for which is assigned specific constitutive laws to describe the material behavior of the layers. In this scope, the fiber orientation profile, fiber segregation and fiber pullout constitutive law were coupled to form a new material model to simulate the nonlinear material behavior of FRC.

For the simulation of the tensile behavior of the FRC, a linear elastic stress-strain response was considered, up to tensile strength, f_{ct}, is reached. For the post-cracking tensile response of FRC, the contribution of the fiber pullout resistance, $P(w)$, was added to the post-cracking residual strength of FRC matrix, $\sigma_{ct}(w)$, namely:

$$\sigma^j = \frac{P^j\left(w^j\right)}{b^j \cdot t^j} + \sigma_{ct}^j\left(w^j\right) \tag{1}$$

where b^j and t^j are, respectively, the width and thickness of the generic j^{th} layer that discretizes the cross-section, and w^j is the crack width at the level of the geometric center of the j^{th} layer.

The adopted stress-crack width relationship of the concrete matrix is based on the model presented in [20].

For the usual fiber dosages used in FRC's, its compressive behavior is similar to the one observed in plain concrete. Therefore, the simulation of the behavior of FRC in compression was done by adopting the model proposed in [17].

2.1 Fiber orientation profile model

The model for predicting the distribution of orientation angles of the fibers, φ_i, is based on the definition of an orientation factor, η. The orientation factor corresponds to the average length of the projection of all fibers crossing a crack plane on its orthogonal direction, divided by the fiber length [18]. The fiber orientation factor can vary between 0.0 and 1.0, corresponding, respectively, to fibers parallel and orthogonal to the analyzed cross-section (herein representing the crack plane) [19]. The fiber orientation factor relates the theoretical number of fibers, N_{th}, contained in the concrete medium with the number of fibers to be encountered in a cross-section, N_f, according to the expression [20]:

$$N_f = N_{th} \cdot \eta = \frac{A_{\text{sec}}}{A_f} \cdot V_f \cdot \eta \tag{2}$$

where A_{sec} is the cross-section area of the FRC element, A_f is the cross sectional area of a fiber, and V_f is the fiber volume dosage.

The fiber orientation profile model is based on the work of [18], where the distribution of the orientation of the fibers in a cross-section is arranged in discrete intervals, $n\Delta\varphi$, and the number of fibers within each orientation angle interval, $N_{f,\overline{\varphi_i}}$ is determined according to the expression:

$$N_{f,\overline{\varphi_i}} = C\left(\overline{\varphi_i}\right) \cdot N_f \tag{3}$$

where $C\left(\overline{\varphi_i}\right)$ is the ratio between the number of fibers within each interval range with a mean orientation angle $\overline{\varphi_i}$ and the total number of fibers in the cross-section. The parameter $C\left(\varphi_i\right)$ can be determined by the expression [18]:

$$C\left(\overline{\varphi_i}\right) = f\left(\overline{\varphi_i}\right) \cdot F_{RE}\left(\eta\right) \tag{4}$$

where $f\left(\overline{\varphi_i}\right)$ is the frequency of fibers within the interval of orientation angles $\varphi_i \pm \Delta\varphi_i/2$, $\Delta\varphi_i = 90/n\Delta\varphi$, considering a Gaussian law to describe the frequency distribution, and $F_{RE}(\eta)$ is a coefficient to account to the error resultant of adopting discrete ranges of fiber orientation angles rather than considering a continuous function, which is determined with Eq. (5).

$$F_{RE} = \begin{cases} 1.29 - 0.38 \cdot \eta & ;\eta < 0.75 \\ 1.0 & ;\eta \geq 0.75 \end{cases} \tag{5}$$

Based on the orientation factor is possible to determine the average orientation angle of the fibers in the cross-section, φ_m, and the corresponding standard deviation, $\sigma(\varphi_m)$, using the following equations [18]:

$$\varphi_m = \arccos(\eta) \cdot 180/\pi \quad [^{\circ}] \tag{6}$$

$$\sigma(\varphi_m) = 90 \cdot \eta \cdot (1-\eta) \quad [^{\circ}] \tag{7}$$

The methodology adopted to determine the fiber orientation factor, η, is based on the work of Krenchel [20] for stiff fibers. Due to the wall effect on the orientation of the fibers, the cross-section of the FRC member is divided in three zones with different orientation factors (Fig. 1). The fiber orientation factor of the cross-section is determined by the expression:

$$\eta = \frac{\eta_1 \cdot (b - l_f) \cdot (h - l_f) + \eta_2 \cdot l_f \cdot \left[(b - l_f) + (h - l_f) \right] + \eta_3 \cdot {l_f}^2}{b \cdot h} \tag{8}$$

where l_f is the length of the adopted fiber type, and $\eta_z\,(z = 1,2,3)$ is the fiber orientation factor for each zone of the cross-section.

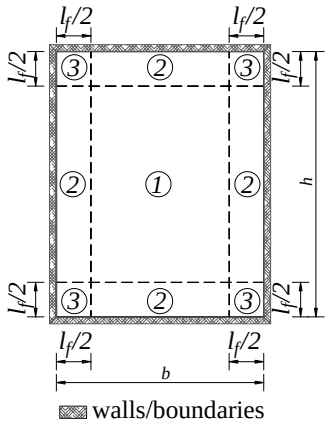

Fig. 1. Zones of cross-section for the determination of the fiber orientation factor due to wall effect.

The values of the orientation factor for each zone of the cross-section are based on previous research, namely: $\eta_1 = 0.50$ [21, 22]; $\eta_2 = 2/\pi$ [22]; $\eta_3 = 0.84$ [21].

2.2 Fiber segregation model

In order to simulate the fiber segregation phenomena that can occur during FRC casting, a segregation model is proposed, that assumes a linear variation of the fiber's distribution along the depth of the cross-section. The model solely defines the segregation factor, ξ, varying between -1.0 to +1.0. Considering the thickness $t^j \left(j = 1,...,N \right)$ and depth of the geometric center of each layer of the cross-section $d^j \left(j = 1,..,N \right)$, the number of fibers in each layer is determined by the following expression:

$$N_f^j = \left(N_f^{top} \left(1 - \frac{d^j}{h} \right) + N_f^{bot} \cdot \frac{d^j}{h} \right) \cdot t^j \; ; \; j = 1,...,N \tag{9}$$

where h is the cross-section height, N_f^{top} and N_f^{bot} are, respectively, the number of fibers at top and bottom faces of the cross-section that are determined according to:

$$N_f^{top} = \frac{N_f}{h} \cdot \left(1 - \xi \right) \tag{10}$$

$$N_f^{bot} = \frac{N_f}{h} \cdot \left(1 + \xi \right) \tag{11}$$

where N_f is the total number of fibers in the cross-section.

For a homogenous distribution of the fibers in the cross-section, the segregation factor assumes a value of $\xi = 0$, and $N_f^{top} = N_f^{bot}$. If $\xi = 1.0$ is assumed, $N_f^{top} = 0$, while $N_f^{bot} = 0$ if $\xi = -1.0$.

2.3 Fiber pullout constitutive model

The considered fiber pullout constitutive model is based on the Unified Variable Engagement Model (UVEM) proposed by [12, 23, 24] for steel fiber reinforced concrete (SFRC). The UVEM combines Mode I and Mode II fracture process of SFRC. The present section presents the main aspects of the proposed model, while further details can be obtained elsewhere [15].

The proposed model adopts an uniform bond strength, τ_b, along the fiber embedded length that is a function of the slip displacement of the fiber. The adopted bond strength vs. slip model ($\tau_{b,0} - \delta$), illustrated in Fig. 2a, is idealized for the pullout response of an aligned fiber ($\varphi = 0^o$). The bond strength vs. slip model is defined by the following four parameters (Fig. 2a and Eq. (12)): the peak bond strength, $\tau_{b,o,p}$; the slip corresponding to the peak bond strength, δ_p; and the exponents α and β, which define the $\tau_{b,0} - \delta$ variation in its pre-peak and post-peak stage.

$$\tau_{b,o} = \begin{cases} \tau_{b,0,p} \cdot \left(\dfrac{\delta}{\delta_p} \right)^{\alpha} & \delta \le \delta_p \\ \tau_{b,0,p} \cdot \left(\dfrac{\delta}{\delta_p} \right)^{-\beta} & \delta > \delta_p \end{cases} \tag{12}$$

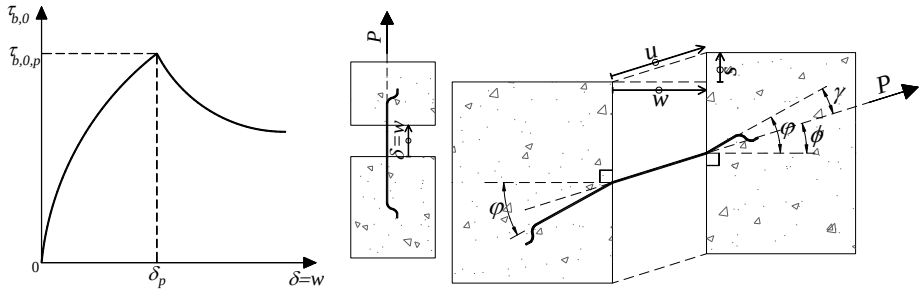

a) b)

Fig. 2. a) Idealized bond stress vs. slip ($\tau_{b,0} - \delta$) for the pullout response of an aligned fiber. b) Definition of fiber bending angle, γ.

In order to consider the snubbing effect in the pullout resistance of the fiber, the expression presented in [24] is adopted:

$$\tau_b(\delta) = \tau_{b,0}(\delta) + 0.25 \cdot \gamma^3 \tag{13}$$

where γ is the fiber bending angle, being defined as the angle between the fiber longitudinal axis and pullout force direction (Fig. 2b). For Mode I fracture, fiber bending angle is equal to the fiber orientation angle ($\gamma = \varphi$).

The model admits that all the fiber slippage from the matrix occurs from the shorter embedded length of the fiber, and the slip between the longer embedded part of the fiber and its surrounding matrix is negligible. This assumption leads to the slip of the shorter embedded length being equal to the crack opening displacement of the cimentitious matrix. As illustrated in Fig. 3, the pullout force of a fiber with an orientation angle φ_i, P_{φ_i}, corresponding to a crack opening displacement, w, is equal to:

$$P_{\varphi_i}(w) = \cdot\pi \cdot d_f \cdot \tau_b(\varphi_i, \delta = w) \cdot L_{bf,o}(w) \tag{14}$$

where d_f is the diameter of the fibers; τ_b is the average fiber bond strength determined according to Eq. (13), function of the crack width and orientation angle of the fiber; $L_{bf,o}$ is the fiber embedment length that is equal to its initial value minus the crack opening displacement. For the initial value of the fiber embedment length, which corresponds to a crack width equal to zero ($w = 0$), it is assumed that $L_{bf,o} = l_f / 4$ for the shortest embedment side, considering that it has been verified to be the average length of embedment of the fibers according to the work of [25].

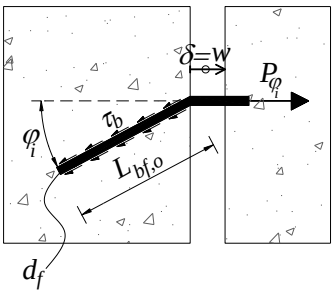

Fig. 3. Pullout force of a fiber with the orientation φ_i.

During the pullout process, fibers may be susceptible to rupture, particularly in the case of the most inclined fibers. The present model considers that a fiber rupture if the tensile stress, σ_f, reaches the effective ultimate tensile strength of the fiber, $\overline{\sigma_{fu}}$. The effective ultimate tensile strength of the fibers is determined through the expression considered in the UVEM model, namely [24]:

$$\overline{\sigma_{fu}} = \sigma_{fu} \cdot \frac{\pi}{2 \cdot \gamma_{\max}} \tag{15}$$

where σ_{fu} is the fiber tensile strength.

The failure criterion of the fibers with circular (or equivalent circular in case o non perfectly circular, such is the case of the adopted PP fibers in the present work) cross-section is verified by the following expression:

$$\overline{\sigma_{fu}} \geq \sigma_f = \frac{4 \cdot \tau_b \cdot L_{bf,o}(w)}{d_f} \tag{16}$$

Considering that the cross-section of a FRC member is discretized in N layers ($j = 1,...,N$), and that the fiber orientation domain is divided into $n\Delta\varphi$ intervals, at the j^{th} cracked layer, the pullout resistance is equal to:

$$P^j(w) = \sum_{i=1}^{n\Delta\varphi} P^j_{\overline{\varphi_i}}(w) \tag{17}$$

$$P^j_{\overline{\varphi_i}}(w) = N^j_{f,\overline{\varphi_i}} \cdot \pi \cdot d_f \cdot \tau_{bu,i} \cdot L_{bf,o}(w) \tag{18}$$

where $P^j_{\overline{\varphi_i}}(w)$ is the pullout resistance of the $N^j_{f,\overline{\varphi_i}}$ fibers with a mean orientation angle $\overline{\varphi_i}$ at the j^{th} cracked layer, determined according to the fiber orientation and segregation models.

3 Assessment of the predictive performance of the model

The predictive performance of the proposed model is assessed by comparing the flexural response of polypropylene fiber reinforced concrete (PPFRC) notched beams submitted to 3-point bending tests, according to [26], with the numerical response determined with software *DOCROS*. Although the proposed numerical model was originally proposed to simulate the flexural behavior of steel fiber reinforced concrete elements, this research work verifies if it has potential to be applicable to other non-metallic discrete fibers reinforcements in concrete.

The PPFRC composition presented in Table 1 was considered, while two mixes with different fiber reinforcement dosages were studied: 6.0 and 3.0kg/m^3.

A new type of PP fibers for structural reinforcement that is being developed in the scope of a R&D project carried out by *Exporplás* and *CiviTest*, is used, which has 0.7mm of equivalent diameter, length equal to 54mm, modulus of elasticity of 6GPa and ultimate tensile strength of 500MPa.

Table 1. PPFRC mix composition.

Portland cement CEM I 52.5R [kg/m^3]	Fly ash [kg/m^3]	Aggregate 6/14mm [kg/m^3]	Aggregate 0/4mm [kg/m^3]	Aggregate 0/2mm [kg/m^3]	Superplasticizer [l/m^3]	Water [l/m^3]
330.0	20.0	750.0	885.0	300.0	7.2	140.0

In order to characterize the relevant mechanical properties of both PPFRC mixes that were considered in this study, an experimental program was carried out to determine the concrete compressive strength (NP EN 12390-3:2009[27]), modulus of elasticity (NP EN 12390-13:2013 [28]) and post-cracking residual flexural strength (EN 14651:2005 [26]) at the age of 28 days. The results of the mechanical characterization of the PPFRC are summarized in Table 2.

Table 2. Average values of the mechanical properties of the PPFRC mixes (Legend: † - Coefficient of variation).

Mixture	f_{cm} [MPa]	E_{cm} [GPa]	f_{Lm} [MPa]	f_{R1m} [MPa]	f_{R2m} [MPa]	f_{R3m} [MPa]	f_{R4m} [MPa]
Mix with 6kg/m^3 of PP fibers	35.1 (1%)†	24.9 (4%)†	3.25 (7%)†	1.88 (20%)†	1.97 (26%)†	2.04 (27%)†	2.07 (27%)†
Mix with 3kg/m^3 of PP fibers	33.4 (1%)†	25.6 (1%)†	3.70 (7%)†	1.48 (21%)†	1.41 (30%)†	1.44 (34%)†	1.40 (31%)†

Since at the present stage of the research activities, the local bond-slip relationship (Fig. 2a) of the used PP fibers are not yet available from experimental tests (by adopting inverse analysis with the results from fiber pullout tests), the parameters that define this local law were obtained by a fitting procedure implemented in *DOCROS*, that resorts to the nonlinear least squares fitting routine *MPFIT* [29]. The data considered in the fitting procedure corresponded to the average of the moment vs. crack tip opening displacement (CTOD) relationship that was derived from the experimental results of 3 samples submitted to the bending tests.

Fig. 4a and 4b present the comparison between the experimental and numerical response of the force vs. CTOD relationship of the PPFRC prisms submitted to 3-point bending, while Fig. 4c presents the bond stress vs. slip relationship, $\tau_{b,0} - \delta$, for the pullout response of the aligned PP fibers obtained by the fitting procedure, for each PPFRC mix. As demonstrated in Fig. 4, the proposed model captures with very good agreement the flexural behavior of the PPFRC prisms.

To be noticed that the derived peak bond strength of pullout response of fibers is dependent on the fiber dosage of the PPFRC, with the peak bond strength being inversely proportional to the employed fiber dosage. This phenomenon points to a detrimental effect of the increased number of fibers on the pullout response of each individual fiber.

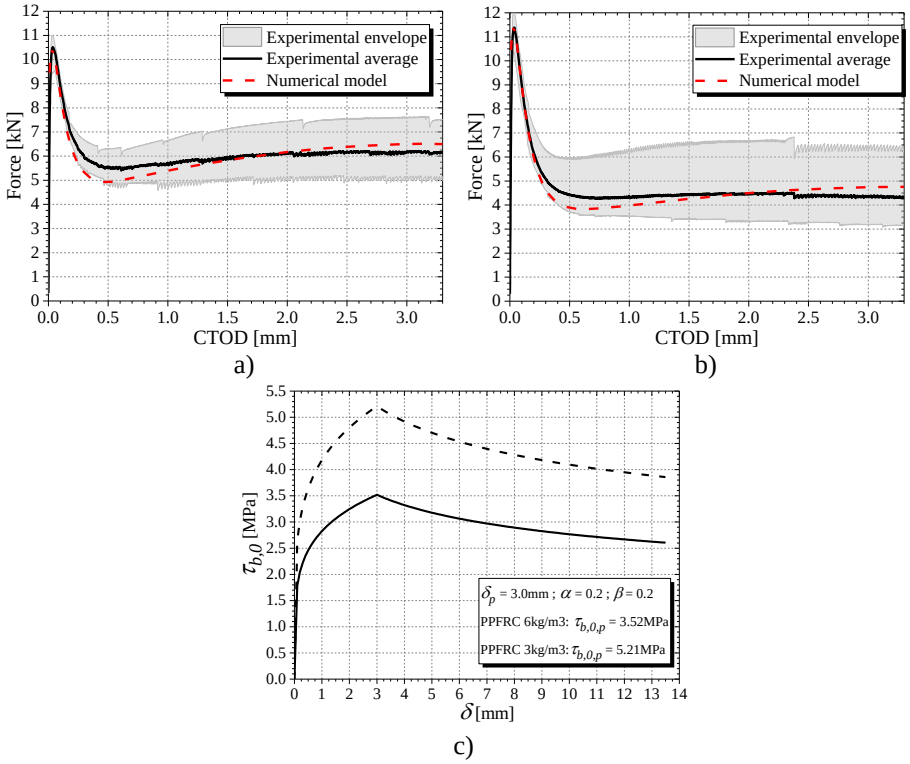

Fig. 4. Experimental and numerical model comparison of force vs. CTOD relationship for PPFRC with: a) 6kg/m^3 of PP fibers; b) 3kg/m^3 of PP fibers; c) Derived bond stress vs. slip ($\tau_{b,0} - \delta$) of the pullout response of the aligned PP fibers.

4 Conclusions

This study presents a new integrated model capable of describing the flexural behavior of 1D type FRC members considering the orientation of the fibers, the fiber segregation along the cross-section of these members, and the pullout constitutive model of each fiber bridging the two faces of a crack.

Nonetheless the proposed numerical model has been originally developed to simulate the behavior of steel fiber reinforced concrete, it is shown that it can also capture with very satisfactory accuracy the behavior of concrete reinforced with non-metallic discrete fibers, as is the case of the studied PP fibers.

The accuracy of the model would greatly benefit from the characterization of the pullout response of aligned and inclined fibers, including a more in-depth study regarding the influence of the number of fibers bridging a crack on the pullout response of each individual fiber.

For the particular case of members made by concrete reinforced with flexible fibers such is the case of PP fibers), an upgrade to the fiber orientation and distribution model is under development, which will also contribute to improve the predictive

performance of the integrated model to simulate the flexural behavior of PPFRC members.

Acknowledgements

The authors would like to acknowledge the support provided by *Exporlás*, regarding the provision of the PP fibers to conduct the study. This work is supported by the European Regional Development Fund (FEDER) through the Competitiveness and Internationalization Operational Program – COMPETE under the NG_TPfib project POCI-01-0247-FEDER-033719.

5 References

1. Barros JAO (1995) Comportamento do betão reforçado com fibras - análise experimental e simulação numérica / Behavior of fiber reinforced concrete - experimental and numerical analysis. PhD Thesis, Department of Civil Engineering, FEUP
2. Barros JAO, Sena-Cruz J (2001) Fracture energy of steel fiber-reinforced concrete. Mech Compos Mater Struct 8:29–45
3. Brandt AM (2009) Cement based composites: materials, mechanical properties, and performance, 2nd ed. Taylor & Francis, Milton Park, Abingdon, Oxon
4. Banthia N (1994) Fiber reinforced concrete. ACI SP-142ACI Detroit MI 91–119
5. Mazaheripour H, Barros JAO, Soltanzadeh F, Sena-Cruz J (2016) Deflection and cracking behavior of SFRSCC beams reinforced with hybrid prestressed GFRP and steel reinforcements. Eng Struct 125:546–565 . https://doi.org/10.1016/j.engstruct.2016.07.026
6. Frazão C, Barros J, Camões A, Alves AC, Rocha L (2016) Corrosion effects on pullout behavior of hooked steel fibers in self-compacting concrete. Cem Concr Res 79:112–122 . https://doi.org/10.1016/j.cemconres.2015.09.005
7. Ferrara L, Meda A (2007) Relationships between fibre distribution, workability and the mechanical properties of SFRC applied to precast roof elements. Mater Struct 39:411–420 . https://doi.org/10.1617/s11527-005-9017-4
8. Ferrara L, Park Y-D, Shah SP (2008) Correlation among fresh state behavior, fiber dispersion, and toughness properties of SFRCs. J Mater Civ Eng 20:493–501
9. Stähli P, Custer R, van Mier JGM (2008) On flow properties, fibre distribution, fibre orientation and flexural behaviour of FRC. Mater Struct 41:189–196 . https://doi.org/10.1617/s11527-007-9229-x
10. Abrishambaf A, Cunha VMCF, Barros JAO (2015) The influence of fibre orientation on the post-cracking tensile behaviour of steel fibre reinforced self-compacting concrete. Fract Struct Integr J Volume 31:38–53
11. Vítor M. C. D. Cunha, Joaquim A. O. Barros, José M. Sena-Cruz (2010) Pullout Behavior of Steel Fibers in Self-Compacting Concrete. J Mater Civ Eng 22:1–9 . https://doi.org/10.1061/(ASCE)MT.1943-5533.0000001
12. Ng TS, Foster SJ, Htet ML, Htut TNS (2014) Mixed mode fracture behaviour of steel fibre reinforced concrete. Mater Struct 47:67–76 . https://doi.org/10.1617/s11527-013-0045-1

13. Voo JYL, Foster SJ (2004) Tensile-fracture of fibre-reinforced concrete: Variable Engagement Model. In: Sixth RILEM Symposium on Fibre-Reinforced Concrete (FRC) - BEFIB 2004. RILEM, Varenna, Italy, pp 874–884
14. Htut TNS, Foster SJ (2010) Unified model for mixed mode fracture of steel fibre reinforced concrete. In: Proceedings of the 7th International Conference on Fracture Mechanics Concrete and Concrete Structures (FramCoS-7). Jejyu, Korea, pp 1469–1477
15. Tiago Valente (2019) Advanced tools for design and analysis of fiber reinforced concrete structures. PhD Thesis, University of Minho
16. Häßler D, Barros, J.A.O Exploring the possibilities of steel fibre reinforced self-compacting concrete for the flexural strengthening of masonry structural elements. Int J Archit Herit Conserv Anal Restor 26–53
17. Barros JAO, Varma RK, Sena-Cruz JM, Azevedo AFM (2008) Near surface mounted CFRP strips for the flexural strengthening of RC columns: Experimental and numerical research. Eng Struct 30:3412–3425 . https://doi.org/10.1016/j.engstruct.2008.05.019
18. Laranjeira de Oliveira F (2010) Design-oriented constitutive model for steel fiber reinforced concrete. PhD Thesis, Universitat Politècnica de Catalunya
19. Laranjeira F, Aguado A, Molins C, Grünewald S, Walraven J, Cavalaro S (2012) Framework to predict the orientation of fibers in FRC: A novel philosophy. Cem Concr Res 42:752–768 . https://doi.org/10.1016/j.cemconres.2012.02.013
20. Krenchel H- (1975) Fibre spacing and specific fibre surface. In: Proceedings of Rilem Symposium on Fibre Reinforced Cement and Concrete. Construction press, pp 69–79
21. Dupont D, Vandewalle L (2005) Distribution of steel fibres in rectangular sections. Cem Concr Compos 27:391–398 . https://doi.org/10.1016/j.cemconcomp.2004.03.005
22. Alberti MG, Enfedaque A, Gálvez JC (2017) On the prediction of the orientation factor and fibre distribution of steel and macro-synthetic fibres for fibre-reinforced concrete. Cem Concr Compos 77:29–48 . https://doi.org/10.1016/j.cemconcomp.2016.11.008
23. Htut T, Foster SJ (2012) Fracture of steel fibre reinforced concrete - the unified variable engagement model. The University of the New South Wales, UNSW Sydney, Australia
24. Htut T (2010) Fracture processes in steel fibre reinforced concrete. PhD Thesis, School of Civil and Environmental Engineering, The University of New South Wales, UNSW Sydney
25. Marti P, Pfyl T, Sigrist V, Ulaga T (1999) Harmonized test procedures for steel fibre-reinforced concrete. ACI Mater J 96:676–685
26. European Committee for Standardization (2005) Test method for metallic fibered concrete - Measuring the flexural tensile strength (limit of proportionality (LOP), residual)
27. European Committee for Standardization (2009) Testing hardened concrete - Parte 3: Compressive strength of test specimens
28. European Committee for Standardization (2013) Testing hardened concrete – Part 13: Determination of secant modulus of elasticity in compression
29. Markwardt CB (2009) Non-linear least squares fitting in IDL with MPFIT. In: Astronomical Data Analysis Software and Systems XVIII. ASP Conference Series, Quebec, Canada, pp 251–254